Audio Engineering Society

Convention Paper 9839

Presented at the 143rd Convention
2017 October 18–21, New York, NY, USA

Variable Fractional Order Analysis of Loudspeaker Transducers: Theory, Simulations, Measurements, and Synthesis

Andri Bezzola[1], Pascal Brunet[1], and Shenli Yuan[2]

[1]*Samsung Research America, DMS Audio, Valencia CA 91355*
[2]*CCRMA, Stanford University, Stanford CA 94305*

Correspondence should be addressed to Andri Bezzola (andri.b@samsung.com)

ABSTRACT

Loudspeaker transducer models with fractional derivatives can accurately approximate voice coil inductance over a wide frequency band. Analytical solutions to Maxwell equations in infinite lossy coils can be interpreted as fractional derivative models. However, they suggest that fractional order α cannot be a constant, but rather a function of frequency that takes on values between 1/2 and 1. Finite Element simulations bridge the gap between the theoretical first-principles approach and lumped parameter models using fractional derivatives. This work explores the dependence of α on frequency for infinite and finite cores as well as in transducers. To better match the measured impedances and frequency-dependent α values, we propose to represent the voice coil impedance by a cascade of R-L sections.

1 Introduction

In its simplest form, a loudspeaker's blocked voice coil impedance Z can be approximated by resistor connected in series with an inductor. The electric impedance of the resistor R_{DC} is real and constant over the frequency range. An ideal inductor has an impedance that is linearly proportional to the applied angular frequency ω. However, measurements show a more complex relationship for Z. In its most general form it can be written as $Z(\omega) = R_{DC} + Z_{AC}(j\omega)$, with $Z_{AC}(\cdot)$ any complex function. Analytical solutions for infinite lossy coils show that $Z_{AC}(j\omega)$ is proportional to $\Lambda(j\omega)^{\alpha}$ with Λ a complex constant and $\alpha = 0.5$ above a certain transition frequency, and $\alpha = 1$ below the transition frequency. Between the two limits, there is a rather narrow transition band [1]. Measurements of loudspeaker transducers suggest that the transition period is much wider and the limiting values of $\alpha = 1$ and $\alpha = 1/2$ lie typically outside the audio band. For practical engineering purposes, many lumped parameter models have been derived to approximate $Z_{AC}(j\omega)$ of transducers by means of curve fitting [2, 3, 4, 5]. The accuracy of these models is typically restricted to a limited subset of the audio band. Recently, mathematical models involving fractional derivatives have emerged to promise a better fit for a larger bandwidth

with fewer parameters [6, 7, 8]. These models are similar in structure to the analytic solution for infinite coils $Z = R_{DC} + \Lambda(j\omega)^{\alpha}$, but they allow the constant parameter α, the fractional order, to take on any real value between 0.5 and 1. The value of α can again be found by means of curve fitting.

All these fitting models can be useful for engineers to infer certain characteristics of their loudspeaker motor design, but they lack a direct link to a tangible physical explanation of the observed impedance function. On the other hand, the theoretical physical models can only be solved for a restricted number of geometries due to the difficulty to find analytic solutions with proper boundary conditions. Numerical modeling techniques, such as Finite Element Models (FEM), bridge the gap between theory and experiment, because they can solve the approximations of the Maxwell equations with real-world geometries and proper boundary conditions. These methods have been around long enough to find their use in loudspeaker transducer simulations. In particular the blocked voice coil simulation has been extensively used to evaluate and improve transducer designs [3, 9, 10, 11, 12].

In this paper, FEM is used to first compare its results to analytical solutions. FEM models solve the Maxwell equations by discretization of space and finding piecewise polynomial solutions across the elements. With this model one can show how the impedance of a blocked voice coil transitions from a fractional inductor with $\alpha = 1$ at low frequencies to $\alpha = 0.5$ at high frequencies if the geometry is an infinitely long core with a coil carrying a current flowing in azimuthal direction (see Figure 1). We show how the dependence of α on the frequency ω changes if the geometry is changed to a finite length. Finally we model several real-world transducer geometries and determine their blocked voice coil impedance based on geometry and material data. From these simulations we can extract the fractional order α as a function of frequency, and we show how it varies across the frequency spectrum, suggesting that fractional derivative models should not be approximated with a constant α if they operate over a wide bandwidth. Finally, we propose to synthesize the voice coil impedances by a cascade of R-L sections to better match the measurement data. This representation can be used in the frequency and time domains - a great benefit if the transducers are to be electronically controlled.

2 Analytic Solutions

2.1 Fractional Order α

As mentioned in the introduction, a blocked coil's complex impedance Z can be thought of as a combination of the static resistance R_{DC} and a dynamic complex part Z_{AC} that is a function of frequency:

$$Z = R_{DC} + Z_{AC}(j\omega) \in \mathbb{C}. \tag{1}$$

It is the subject of this work to analyze and characterize the complex dynamic part of the impedance. Fractional derivative models suggest that writing Z_{AC} as a power α ($\alpha \in \mathbb{R}$) of $j\omega$ can provide good agreement between model and measurements:

$$Z = R_{DC} + \Lambda \cdot (j\omega)^{\alpha}, \tag{2}$$

where Λ is a complex constant. If this were exact, then a log-log plot of the magnitude of $Z - R_{DC}$ versus frequency would result in a straight line with slope α. To see this, one can write $log(|Z - R_{DC}|)$. After some manipulation and using $\omega = 2\pi f$:

$$\begin{aligned} log(|Z - R_{DC}|) &= log(|\Lambda \cdot (j\omega)^{\alpha}|) \\ &= log(|\Lambda|) + \alpha \cdot log(\omega), \end{aligned} \tag{3}$$

which is a straight line in the log-log plot that crosses the point $|\Lambda|$ at $\omega = 1$ rad/s, and has a constant slope of α.

However, in 1989 Vanderkooy postulated that loudspeaker voice coils should show a magnitude of the AC impedance that is proportional to $j\omega$ at low frequencies and proportional to $\sqrt{j\omega}$ at high frequencies with a transition period in between. He derived this postulation from analytic equations for an infinitely long magnetic cores with an infinitely thin sheet of current flowing in circumferential direction around it [1]. This postulation stands in contrast with the fractional derivative assumption, because it means that a log-log plot of $|Z - R_{DC}|$ vs. frequency would have a slope of 1 at low frequencies and a slope of 1/2 at high frequencies.

Vanderkooy obtained his result by solving the Maxwell equations on the simplified geometry of an infinite coil that has a turn density of n turns per unit length of core and that carries a current I_{ϕ}. The core material can be defined electromagnetically by the following parameters: the permeability μ (often given as the relative permeability $\mu_r = \mu/\mu_0$, with μ_0 the permeability

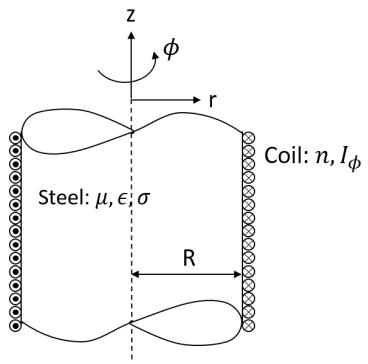

Fig. 1: A diagram of the infinite coil around an infinite core. The core has radius R and its material properties are given by μ, ε, and σ. The coil is infinitely thin and carries a current in the ϕ-direction with a turn density of n turns per unit length of the core. The core's axis lines up with the z-axis, and the sign of ϕ is given by the right-hand rule.

of vacuum $4\pi \cdot 10^{-7}$ H/m), the permittivity ε (often given as the relative permittivity $\varepsilon_r = \varepsilon/\varepsilon_0$, with ε_0 the permittivity of vacuum $8.85 \cdot 10^{-12}$ F/m), and the electrical conductivity σ. A section of the infinite coil around an infinite core is shown in Figure 1.

This work proposes to relax the constant value of α to a frequency dependent $\alpha(\omega)$. A formula for $\alpha(\omega)$ can be obtained directly from Equation (3) by taking the partial derivative of $log(|Z - R_{DC}|)$ with respect to $log(\omega)$:

$$\alpha(\omega) = \frac{\partial\{log(|Z - R_{DC}|)\}}{\partial\{log(\omega)\}}. \tag{4}$$

2.2 Maxwell's Equations

Maxwell's equations are given as:

$$\vec{\nabla} \times \vec{E} = -\frac{\partial \vec{B}}{\partial t} \tag{5}$$

$$\vec{\nabla} \times \vec{H} = \vec{J} + \cancelto{\sim 0}{\frac{\partial \vec{D}}{\partial t}} \tag{6}$$

Where $\vec{E}$ is the electric potential, $\vec{B}$ is the magnetic flux density, $\vec{H}$ is the magnetic field strength, $\vec{J}$ is the current density, and $\vec{D}$ is the displacement current density. The last term in equation (6) is put to zero in our case because it is an order of $\varepsilon\omega/\sigma$ smaller than J. In steel ε is of order 10^{-11}, σ is of order 10^7, and the highest frequencies in the audio band are of order 10^5. So $\partial\vec{D}/\partial t$ is at least an order 10^{-13} smaller than J, and the displacement currents are thus negligible at these frequencies.

Conservation of charge and non-divergence of the magnetic field lines leads to:

$$\vec{\nabla} \cdot \vec{E} = 0 \tag{7}$$

$$\vec{\nabla} \cdot \vec{B} = 0. \tag{8}$$

And finally the current density is linked to the electric potential as

$$\vec{J} = \sigma\vec{E} \tag{9}$$

and the magnetic flux density is coupled to the magnetic field strength as

$$\vec{B} = \mu\vec{H}. \tag{10}$$

Combining these equations and using the vector identity $\vec{\nabla} \times (\vec{\nabla} \times \vec{H}) = \vec{\nabla}(\vec{\nabla} \cdot \vec{H}) - \nabla^2\vec{H}$ one can arrive at the diffusion equation for the magnetic field:

$$\nabla^2\vec{H} = \mu\sigma\frac{\partial \vec{H}}{\partial t}. \tag{11}$$

In the case of an infinite cylinder of constant cross section, (11) further reduces from three dimensions to a single dimension

$$\frac{\partial^2 H_z}{\partial r^2} + \frac{1}{r}\frac{\partial H_z}{\partial r} = \mu\sigma\frac{\partial H_z}{\partial t}. \tag{12}$$

Under the assumption of harmonic time dependence and separation of variables, $H_z(r,t)$ can be written as

$$H_z(r,t) = H_z(r)e^{j\omega t}. \tag{13}$$

Plugging this assumption into equation (12) we end up with the following ordinary differential equation in r:

$$\frac{\partial^2 H_z(r)}{\partial r^2} + \frac{1}{r}\frac{\partial H_z(r)}{\partial r} = j\mu\sigma\omega H_z(r). \tag{14}$$

Using the definition of the skin depth

$$\delta = \sqrt{\frac{2}{\mu\sigma\omega}}, \tag{15}$$

the solution to equation (12) can then be written as

$$H_z(r,t) = H_0 \frac{\mathbf{I_0}\left(\frac{r}{\delta}(1+j)\right)}{\mathbf{I_0}\left(\frac{R}{\delta}(1+j)\right)} e^{j\omega t} \tag{16}$$

where $\mathbf{I_0}$ consists of the modified Bessel functions of the first kind and order zero and R is the core radius.

In order to get to the current density inside the core, we use (6) for the axisymmetric case of an infinite cylinder. While the magnetic field only has a component in z-direction, the current density only has a component in the ϕ-direction.

$$J_\phi = -\frac{\partial H_z}{\partial r}, \tag{17}$$

so J_ϕ can be calculated as

$$J_\phi(r,t) = -H_0 \frac{(1+j)}{\delta} \frac{\mathbf{I_1}\left(\frac{r}{\delta}(1+j)\right)}{\mathbf{I_0}\left(\frac{R}{\delta}(1+j)\right)} e^{j\omega t}. \tag{18}$$

Finally, the value of the field at the cylinder surface, H_0, is linked to the applied current as

$$H_0 = nI_\phi \tag{19}$$

where the applied current I_ϕ runs through a coil with n turns per unit length of the core.

The total magnetic flux per unit length Φ can be calculated by integrating $\mu H_z(r,t)$ over the core cross section and multiplying it with the turn density n:

$$\begin{aligned} \Phi &= 2\pi n\mu \int_0^R H_z(r,t) r\, dr \\ &= \pi n\mu H_0 R\delta(1+j) \left[\frac{\mathbf{J_1}\left(\frac{R}{\delta}(1+j)\right)}{\mathbf{J_0}\left(\frac{R}{\delta}(1-j)\right)}\right], \end{aligned} \tag{20}$$

with $\mathbf{J_1}$ the Bessel function of the first kind of order one. Combine this result with the definition of inductance L per unit length:

$$\begin{aligned} L &= \frac{\Phi}{I_\phi} \\ &= \pi n^2 \mu R\delta(1+j) \left[\frac{\mathbf{J_1}\left(\frac{R}{\delta}(1-j)\right)}{\mathbf{J_0}\left(\frac{R}{\delta}(1-j)\right)}\right]. \end{aligned} \tag{21}$$

Now the AC impedance per unit length can finally be written as

$$\begin{aligned} Z &= L\, j\omega \\ &= \pi n^2 \mu R\delta\omega(j-1) \left[\frac{\mathbf{J_1}\left(\frac{R}{\delta}(1-j)\right)}{\mathbf{J_0}\left(\frac{R}{\delta}(1-j)\right)}\right]. \end{aligned} \tag{22}$$

For low frequencies, the term inside the square brackets can be expanded to

$$[\cdot]\Big|_{\omega\to 0} = \frac{R}{2\delta}(1-j) + \mathscr{O}\left(\left(\frac{R}{\delta}\right)^3\right). \tag{23}$$

At high frequencies, the asymptote of the square bracket tends to $-j$:

$$\lim_{\omega\to\infty}[\cdot] = -j. \tag{24}$$

Substituting (23) back into (22), and ignoring the higher order terms, we arrive at:

$$Z = j\omega[\mu n^2 \pi R^2] = j\omega[\mu n^2 A] \tag{25}$$

where A is the cross-sectional area of the solenoid. Setting the term in brackets equal to an inductance, L:

$$L = \mu n^2 A \tag{26}$$

which is the formula for the inductance per-unit length of a solenoid. This makes sense for the low-frequency limit.

For high frequencies, substituting (24) into (22), we arrive at:

$$Z = \sqrt{\frac{\omega\mu}{\sigma}}[n^2 2\pi R]\left(\frac{1+j}{\sqrt{2}}\right) \tag{27}$$

The impedance varies as $\sqrt{\omega}$ and has equal real and imaginary parts, and $+45^\circ$ phase shift at all (high) frequencies. Because at high frequencies the flux is confined to the surface of the cylinder, it is not surprising to see the circumference $C = 2\pi R$ in the expression. The last equation can also be written as:

$$Z = \sqrt{j\omega}\sqrt{\frac{\mu}{\sigma}}[n^2 2\pi R] \tag{28}$$

where the dependence on $\sqrt{j\omega}$ is shown explicitly.

3 Finite Element Simulations

While it is not impossible to derive analytic solutions for slightly more complex situations, such as the calculation of eddy currents in a conducting rod of infinite or finite length by a fininte size coaxial encircling coil [13, 14], it is rather infeasible to attempt an analytical approach for modern loudspeaker transducer geometries. Engineers have long ago started using numerical

modeling techniques such as FEM to calculate approximate solutions for the Maxwell equations. In this paper, FEM was used to calculate the AC impedance for finite coils and several loudspeaker motors and analyze their fractional order. But first, the FEM modeling technique was validated by approximating the infinite core problem and comparing the FEM solution with the analytical solution.

3.1 Simulation Setup

All FEM simulations have been performed with COMSOL Multiphysics® 5.3 on a desktop computer [15]. We implemented the simulations with the Magnetic Fields environment that is part of the AC/DC module of COMSOL Multiphysics. The Magnetic Fields environment solves the quasi-static Maxwell equations, which are formulated using the magnetic vector potential and, optionally for coils, the scalar electric potential as the dependent variables.

For the approximation of the infinite core and the finite core simulations, it was assumed that the steel material is linear and not magnetized with a relative permeability of $\mu_r = 2100$. For the simulations of the loudspeaker transducers, the non-linear *B-H* relationship of the respective soft magnetic steels was used that can be found in the material library of COMSOL Multiphysics®. The magnet materials in the transducers were assumed to operate in the linear domain well above the demagnetization knee. The voice coils were modeled using the Multiturn Coil feature of the AC/DC Module, which takes coil wire conductivity, number of turns, and wire diameter to model the coil area as a lumped model, without the need to specify each individual turn. Any shorting elements were modeled using the appropriate conductivity, permeability, and permittivity of their respective materials.

Great care was taken to spatially resolve the induced eddy current at high enough resolution. The skin depth for the eddy currents can be estimated using (15). For a typical steel material with $\sigma = 5$ MS/m, and $\mu_r = 2100$, the skin depth at 20 kHz is in the order of $3 \cdot 10^{-5}$ m, and the gradients can be very high. Therefore we carefully selected the mesh to resolve the skin depth at 20 kHz with at least 30 elements. This means that the smallest elements are on the order of one micron at the geometry surface. Such small elements are made possible by the use of boundary mesh elements. For all simulations, we used these thin boundary meshes on all surfaces of conducting components, not only around the voice coil, because plots of the induced currents show skin current occurring on all surfaces, including interfaces between steel, magnets, shorting elements etc.

The simulations of finite cores and loudspeaker transducers require special care at the outer edges of the simulation domain. Infinite elements were employed at these edges to account for the infinite expanse of the air around the samples.

The simulations of infinite and finite cores without static magnetization of permanent magnets were solved using the frequency domain solver. The simulations of the loudspeaker transducers were solved in two steps. The first step solved the static magnetic field that is produced by the permanent magnet. The problem was then linearized around this solution and a frequency domain perturbation solver was employed to solve for the harmonic dynamic field around the linearization point. The linearization can be justified because only the small signal response of a blocked voice coil is of interest in this paper.

3.2 Blocked Voice Coil Measurements

Blocked voice coil measurements were performed to double-check the simulations and to verify that that the FEM models are valid even for magnetized coils. For this paper, four different types of transducers, from subwoofers to tweeters, were simulated with FEM and verified via blocked-coil impedance measurement using the TRF function of the Klippel analyzer. Specifications of the four transducer types are listed in Table 1. The calculation of the fractional order α from measurements is very sensitive to measurement noise at low frequencies where $|Z - R_{DC}|$ is smaller than the measurement error ξ_Z. The error estimate ξ_α for α with respect to the error ξ_Z can be calculated using sensitivity analysis:

$$\begin{aligned} \xi_\alpha &= \left| \frac{d\alpha}{dz} \right| \xi_Z \\ &= \frac{1}{\Delta \log_{10}(f)} \frac{\sqrt{2}}{|Z - R_{DC}|^2} \xi_Z. \end{aligned} \tag{29}$$

The first fraction in (29) is the frequency sampling density as samples per decade. From this equation, it can be seen that the error ξ_α grows with the inverse

Driver Name	A	B	C	D
Transducer Type	Subwoofer	Woofer	Tweeter	Racetrack Driver
VC diameter	2 in	1.5 in	1 in	1 in
Magnet type	Ferrite Y35	Neodymium N42	Neodymium N42	Neodymium N42
DC Resistance	3.3 Ω	3.8 Ω	3.2 Ω	3.8 Ω
Shorting Elements	Al ring below gap	none	none	Cu pole cap

Table 1: Loudspeaker Transducer Specifications

of the square of the measured AC impedance. Since the AC impedance decreases below the measurement accuracy ξ_Z of about 0.01 Ω at low frequencies, ξ_α grows very large for low frequencies. We therefore employed the following sequence of steps to measure and calculate a more accurate estimate of the fractional order at low frequencies:

1. Measure impedance Z_i in 5 samples of each transducer type.
2. Take complex average $\bar{Z} = \frac{1}{5}\sum Z_i$ of these 5 measurements.
3. Smooth the average $\bar{Z}$ using a Savitzky-Golay filter of appropriate length, call this smoothed average $\hat{Z}$.
4. Take the real part of $\hat{Z}$ at 1 Hz as best estimate of R_{DC}.
5. Calculate α using $\hat{Z}$ and the estimated R_{DC} according to Equation (4).

3.3 Results

The FEM simulation method was validated in a first step: A steel core segment of radius R_{core} is capped by perfect magnetic conductor boundaries in axial direction. These boundaries essentially guarantee that the flux inside the core stays parallel to core axis and thus can be used to simulate an infinite core. At the core surface, a current I_ϕ and a turn density n is applied. The core steel is assumed to have a linear relative permeability of $\mu_r = 2100$ and a conductivity of $\sigma = 5$ MS/m. The geometry and setup are shown in Figure 2.

The results for the normalized induced magnetic field strength and normalized induced current density inside a core of 20 mm diameter are shown in Figure 3. The figure also shows a comparison of the FEM results

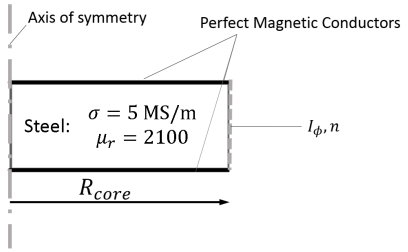

Fig. 2: Simulation setup for the infinite core simulations. The infinite coil is approximated by a short coil with perfect magnetic conductors at the truncations. Mathematically, the perfect magnetic conductors allow magnetic flux lines to start and terminate, which is not possible physically.

with the analytic solutions from (16) and (18). The results show clearly how the magnetic field strength approaches a constant distribution at low frequencies, while at high frequencies the magnetic field is focused inside the skin depth. The current distribution at low frequencies approaches a straight line with zero current on the core axis and maximum current at the core surface. At higher frequencies, the currents are concentrated in the skin are at the core surface, as expected. The FEM simulations and the analytic solutions are in perfect agreement, validating the FEM setup.

Using the validation setup, a core diameter study was performed to see how the impedance is affected by the core diameter. We have simulated and analytically calculated the AC impedance per unit length of the core. Furthermore, the fractional order α as a function of frequency was calculated using (4). The results of this study are shown in Figure 4, and it becomes evident that the frequency where α transitions from 1 to 0.5 is dependent on core diameter as predicted by Vanderkooy. A core of diameter 5 mm and the steel parameters noted above has a transition frequency in

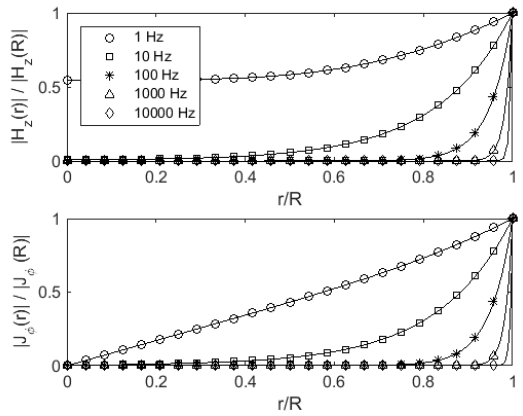

Fig. 3: Comparison of FEM simulation (solid lines) and analytic solution (markers) for the normalized absolute induced magnetic field strength (top) and the normalized absolute induced current density (bottom).

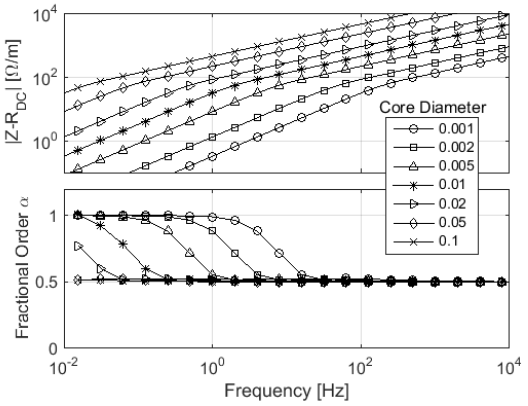

Fig. 4: FEM simulations (solid lines) and analytical solution (markers) for the AC impedance magnitude (top) and the fractional order α (bottom) of infinite coils of different diameters.

the order of 10 Hz, while a core of diameter 50 mm has a transition frequency of about 0.1 Hz. The transition bandwidth is about a decade for all core diameters. These values are much lower than what one observes in measurements of coils of finite lengths, such as are found in moving coil loudspeaker transducers, where α can stay close to 1 for frequencies up to the order of several kilohertz (see Figure 7).

In order to bridge this divide, simulations of cores of finite lengths were performed. The main difference between infinite cores and finite cores is that infinite cores do not have a magnetic field outside the coil, but finite cores do. It is of interest to know how this outside field affects the transition frequency of α from pure inductive to semi-inductive. The results for a core diameter of 20 mm of soft magnetic steel with $\mu_r = 2100$ and $\sigma = 5$ MS/m and a coil with turn density of $n = 5000$ turns per meter are shown in Figure 5. The plot lines for the magnitude of the AC impedance do not exhibit a clear transition from slope of 1 to slope of 1/2; the changes are much more gradual. This is confirmed in the plot of the fractional order for the cores of different lengths. The transition from fully inductive to semi-inductive spans almost 3 decades, or about the bandwidth of human hearing. It is striking, however, how fast the transition frequency increases with decreasing core length. A core of 50 cm has a transition frequency ($\alpha = 0.75$) of 47 Hz, a core of 10 cm has a transition frequency of 3.9 kHz, and a core of 5 cm has a transition frequency of 22 kHz. Cores shorter than 2 cm have transition frequencies above 100 kHz. We note that while all the results shown here are for coils that wrap the entire core, results with shorter coils with turn density n inversely proportional to coil length show the same qualitative AC impedance. The simulated and measured AC impedances of the four different transducers are plotted in Figure 6, and the respective α values are plotted in Figure 7. The AC impedance of Driver D in Figure 6 has been offset by a factor of 100 for better legibility, because its values were similar to the values of transducer B. From these results we can gather that most transducers have a value of α that tends to 1 at low frequencies. Only the subwoofer transducer A appears to not converge towards an ideal inductor. Using simulations down to 1 Hz (not shown here) one can see that even this transducer will eventually converge to $\alpha \approx 1$. For none of the transducers does the fractional order α ever appear to fall outside of 0.5 and 1.

The impedance plots do appear to be close to straight lines for transducers A, B, and C, suggesting that a constant α might be used in fractional order models without incurring a large error. The more rigorous error analysis in the next section and the result for α in Figure 7 shows that α values do change for all transducers. It might be sufficient to assume a constant α if the driver is only used in a narrow band where α has little variation.

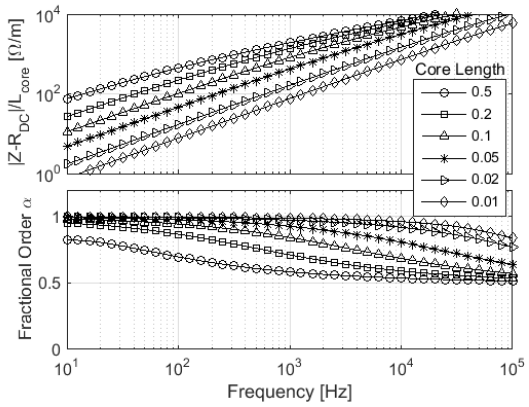

Fig. 5: FEM simulated magnitude of AC impedance (top) and fractional order α for finite coils of different lengths. Shorter coils have higher transition frequencies ($\alpha = 0.75$) than longer coils. The transition bandwidth is roughly 3 decades for all lengths.

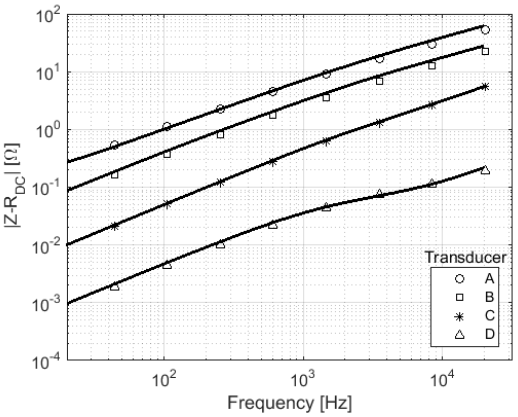

Fig. 6: FEM simulations (solid lines) and measurements (markers) of the AC impedance of Drivers A to D. **Note:** Impedance values of transducer D are plotted lower by a factor of 100 for better legibility.

Transducer D exhibits an interesting curve for α. It dips down to $\alpha = 0.5$ at around 5 kHz and then rises again for higher frequencies to about $\alpha = 0.7$ at 20 kHz. It is unclear yet why and how exactly this is happening, but these kinds of effects are part of ongoing research. This results shows that variable order α will have to be taken into account for certain transducers when they

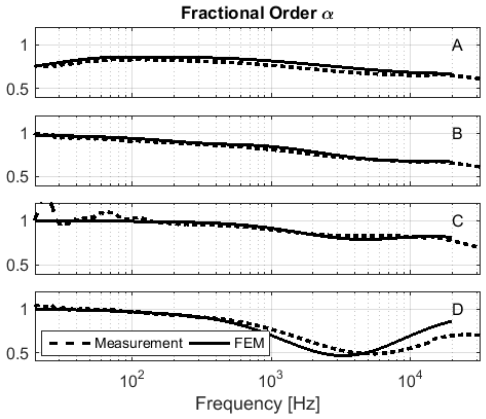

Fig. 7: FEM simulations (solid) and measurements (dotted) of fractional order α of the magnitude of the AC impedance of transducers A to D.

are modeled with fractional order calculus. This is particularly true for full bandwidth transducers. In the next sections, an attempt is made to provide a possible framework to study fractional order models that exhibit variable values of α across the spectrum.

4 NETWORK SYNTHESIS

Experimental data and simulations show that the fractional order inductance model described by (2), although appealing by its simplicity, is insufficient to accurately describe the wideband behavior of loudspeaker transducers. When we compare this model with our measurement data we get errors (RMSE) ranging from 19% to 63% (see table 2, and Figure 8). The RMSE is the Relative Mean Squared Error between measurements and model, calculated in the complex domain:

$$RMSE(Z,\hat{Z}) = \frac{\|\hat{Z} - Z\|}{\|Z\|}. \tag{30}$$

The fractional order inductance model is interesting in the frequency domain, but it is difficult to use in the time domain. Methods exist [16, 17] to approximate an fractional order inductance over a certain bandwidth with a finite integer order filter:

$$\Lambda s^{\alpha} \approx \Lambda \prod_{n=1}^{N} \frac{s + z_n}{s + p_n} \tag{31}$$

where $\{z_n, p_n\}_{n=1}^{N}$ are series of intertwined zeros and poles. This filter can be synthesized with a passive network of R-L cells in series (see Figure 9). The number

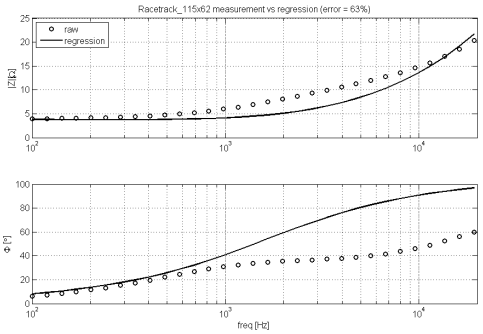

Fig. 8: Driver D - Raw impedance amplitude (top) and phase (bottom) vs. complex regression (i.e. fractional order model).

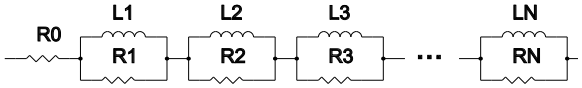

Fig. 9: Equivalent network for voice coil impedance

of cells will determine the bandwidth and accuracy of the approximation. It is clear that the DC resistance of the voice coil can be incorporated in this network without changing its topology. We have here a scalable passive network representation of the blocked voice-coil impedance.

Furthermor,e the element's values can be optimized to match closely the measured impedance. Therefore we propose the following procedure:

1. Collect impedance values Z_{VC} and estimate DC resistance R_{DC}
2. Estimate fractional order exponent α by linear regression in log-log space: $\log(Z_{VC} - R_{DC}) = \alpha \log(\omega) + \beta$
3. Choose approximation bandwidth (e.g. 1-10^5 Hz) and filter order (e.g. $N = 8$)
4. Determine approximation filter (or R-L network values)
5. Optimize filter (or network) values to match measured impedance

Examples show good results with this approach (see Figure 10 and Table 2).

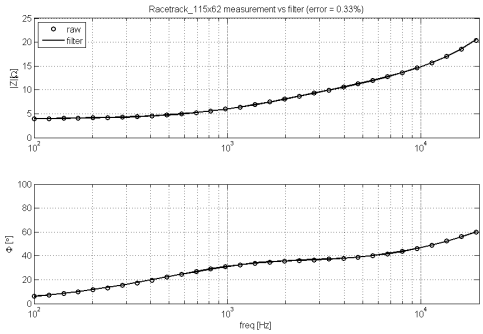

Fig. 10: Driver D - Log-Log plot of raw impedance data vs. optimized filter with 8 *R-L* cells.

Driver	Regression RMSE	Filter RMSE
A	26%	1.8%
B	39%	1.5%
C	19%	0.54%
D	63%	0.33%

Table 2: RMSE values for regression (simple fractional order model) vs. optimized filter with 8 *R-L* cells) .

The final approximation filter or passive network can then be used for modeling and control of loudspeaker in the time domain.

5 Conclusion

The presented work aims to shed some light on fractional orders of lossy coils and loudspeaker transducers. Fractional order models typically assume that the dynamic impedance Z_{AC} is proportional to $(j\omega)^{\alpha}$ with α constant. On the other hand, analytic derivations for lossy coils suggest that fractional order models should have a frequency dependent α with $\alpha = 1$ at the low frequency limit and $\alpha = 1/2$ at the high frequency limit. Analytical solutions for infinite coils have been revisited and FEM models have been used to calculate the frequency dependence of α for finite coils and several loudspeaker transducers, which turns out to be much more gradual than in the case of infinite coils. Still, most wide-range transducers likely incur significant errors if they are attempted to be modeled with fractional order models of constant α. Therefore we propose to represent the voice-coil impedance by a cascade of R-L sections. This can be especially useful for time-domain modeling and control of loudspeakers. The study also

shows that FEM is a valid and valuable tool to predict transducer impedance as well as α.

6 Acknowledgments

Samsung Electronics and Samsung Research America supported this work. The authors would like to thank the entire staff of Samsung's US Audio Lab who helped with the measurement setup, offered insightful suggestions, reviewed the manuscript and contributed to its content.

References

[1] Vanderkooy, J., "A Model of Loudspeaker Driver Impedance Incorporating Eddy Currents in the Pole Structure," *AES J. Audio Eng. Soc.*, 37(3), pp. 119–128, 1989, ISSN 00047554.

[2] Wright, J., "An Empirical Model for Loudspeaker Motor Impedance," *J. Audio Eng. Soc.*, 38(10), pp. 749–754, 1990, ISSN 00047554.

[3] Dodd, M., Klippel, W., and Oclee-Brown, J., "Voice Coil Impedance as a Function of Frequency and Displacement," in *117th AES Conv.*, p. 6178, San Francisco, CA, USA, 2004.

[4] Klippel, W., "Tutorial: Loudspeaker Nonlinearities - Causes, Parameters, Symptoms," *J. Audio Eng. Soc*, 54(10), pp. 907–939, 2006.

[5] Leach Jr., W. M., "Loudspeaker Voice-Coil Inductance Losses: Circuit Models, Parameter Estimation, and Effect on Frequency Response," *J. Audio Eng. Soc.*, 50(6), pp. 442–449, 2002, ISSN 0004-7554.

[6] Brunet, P. and Shafai, B., "Identification of Loudspeakers Using Fractional Derivatives," *J. Audio Eng. Soc*, 62(7/8), pp. 505–515, 2014.

[7] King, A. and Agerkvist, F. T., "State-Space Modeling of Loudspeakers Using Fractional Derivatives," in *Audio Eng. Soc. Conv. 139*, 2015.

[8] King, A. W. and Agerkvist, F. T., "Position Dependence of Fractional Derivative Models for Loudspeaker Voice Coils with Lossy Inductance," in *Audio Eng. Soc. Conv. 142*, 2017.

[9] Voishvillo, A. and Mazin, V., "Finite-Element Method of Modeling of Eddy Currents and Their Influence on Nonlinear Distortion in Electrodynamic Loudspeakers," in *Audio Eng. Soc. Conv. 99*, 1995.

[10] Thorborg, K. and Unruh, A. D., "Electrical Equivalent Circuit Model for Dynamic Moving-Coil Transducers Incorporating a Semi-Inductor," *AES J. Audio Eng. Soc.*, 56(9), pp. 696–709, 2008, ISSN 15494950.

[11] Voishvillo, A. and Kochendörfer, F., "Application of Static and Dynamic Magnetic Finite Elements Analysis to Design and Optimization of Transducers Moving Coil Motors," in *Audio Eng. Soc. Conv. 135*, 2013.

[12] Svobodnik, A., Shively, R., and Chauveau, M.-O., "Multiphysical Simulation Methods for Loudspeakers—Advanced CAE-Based Simulations of Motor Systems," in *Audio Eng. Soc. Conv. 137*, 2014.

[13] Dodd, C. V. and Deeds, W. E., "Analytical Solutions to Eddy-Current Probe-Coil Problems," *J. Appl. Phys.*, 39(6), pp. 2829–2838, 1968, ISSN 0021-8979, doi:10.1063/1.1656680.

[14] Bowler, J. R. and Theodoulidis, T. P., "Eddy currents induced in a conducting rod of finite length by a coaxial encircling coil," *J. Phys. D. Appl. Phys.*, 38(16), pp. 2861–2868, 2005, ISSN 0022-3727, doi:10.1088/0022-3727/38/16/019.

[15] "Comsol Multiphysics v. 5.3," 2017.

[16] Oustaloup, A., Levron, F., Mathieu, B., and Nanot, F. M., "Frequency-band complex noninteger differentiator: Characterization and synthesis," *IEEE Transactions on Circuits and Systems I: Fundamental Theory and Applications*, 47(1), pp. 25–39, 2000.

[17] El-Khazali, R. and Tawalbeh, N., "Realization of Fractional-Order Capacitors and Inductors," in *5th-IFAC Symposium on Fractional Diff. and its Applications*, 4, pp. 4–7, Nanjing, China, 2012.